PluS Nanoparticles as a tool to control the metal complex stoichiometry of a new thio-aza macrocyclic chemosensor for Ag(I) and Hg(II) in water

Gianluca Ambrosi[a], Elisa Borgogelli[a], Mauro Formica[a], Vieri Fusi[a,*], Luca Giorgi[a], Mauro Micheloni[a], Enrico Rampazzo[b], Massimo Sgarzi[b], Nelsi Zaccheroni[b], Luca Prodi[b,**]

[a] Department of Base Sciences and Foundations, Chemistry Section, University of Urbino "Carlo Bo", P.zza Rinascimento 6, I-61029 Urbino, Italy
[b] Dipartimento di Chimica "Giacomo Ciamician", Università degli Studi di Bologna, Via Selmi 2, 40126 Bologna, Italy

ARTICLE INFO

ABSTRACT

We report here the synthesis of a new thio-aza macrocyclic chemosensor based on the 2,5-diphenyl[1,3,4]oxadiazole in which two thioether groups were inserted in a macrocycle with the aim to make it suitable for the coordination of soft and heavy metal ions. In acetonitrile solution, the fluorescence of the chemosensor changes upon addition of different metal ions, such as Cu(II), Zn(II), Cd(II), Pb(II), Hg(II) and Ag(I), that form a not fluorescent M**L** species and a fluorescent M$_2$**L** species characterized also *via* NMR experiments. The hosting of the chemosensor inside the PluS Nanoparticles leads to a high water solubility, allowing to perform the metal detection without the use of additional solvents and also induced an higher selectivity towards Ag(I) and Hg(II). Moreover, it was demonstrated for the first time the possibility to control the stoichiometry of the formed complex upon changing the number of ligands per nanoparticles. To our opinion, this possibility can give an additional tool for the tuning of the affinity and selectivity of the chemosensor that could be of great interest for the design of more and more efficient systems.

© 2014 Elsevier B.V. All rights reserved.

1. Introduction

The development of fluorescent molecular sensors for the detection of a specific analyte is a growing area of chemistry. Their appeal is due to the fact that they offer many advantages in terms of sensitivity, response time and costs with respect to other detection methods, such as the expensive and time-consuming inductively coupled plasma-mass spectroscopy and atomic absorption spectroscopy [1–4]. Among the possible substrates, metal ions have a central role since they are almost ubiquitous in the functions governing life. Therefore, their selective detection and quantification rises considerable attention in many fields such as environmental and security monitoring, waste management, nutrition, and clinical toxicology [1–7]. In particular, soft and heavy metal ions such as Ag$^+$, Hg^{2+}, Cd^{2+}, and Pb^{2+} presenting a toxic impact on human health [8–11], catalyze great research efforts worldwide towards the design of sensors for their detection in real matrices.

In particular, silver is widely used in the electrical, photographic and imaging industry, as well as in pharmacy [12–14], and it is known to inhibit the activity of many bacteria, viruses, and fungi [15–17]. It is toxic and undergoes bioaccumulation; for example, silver ion inactivate sulfhydryl enzymes and in combination with several metabolites, cause serious environmental and health problems [18,19]. Mercury is one of the most toxic metals; nevertheless it is always present in the lithosphere and in waters due to its widespread use in industry and agriculture. Because of its high affinity for sulphur atoms it strongly interacts with many proteins and enzymes thus bioaccumulating and producing pathological diseases [20,21]. Similarly, the presence of cadmium and lead in several industrial processes and devices (for example in batteries) increases the possible exposure to these elements with serious fallouts for human health (inducing memory loss, anaemia, muscle paralysis, and mental retardation) and for the environment [22].

In this context, we have recently reported the synthesis and study of the binding properties of a class of macrocyclic chemosensors based on polyamines as coordinating groups and the 2,5-diphenyl[1,3,4]oxadiazole (PPD) as signalling unit incorporated in the macrocyclic skeleton [23,24]. The ligand shows four
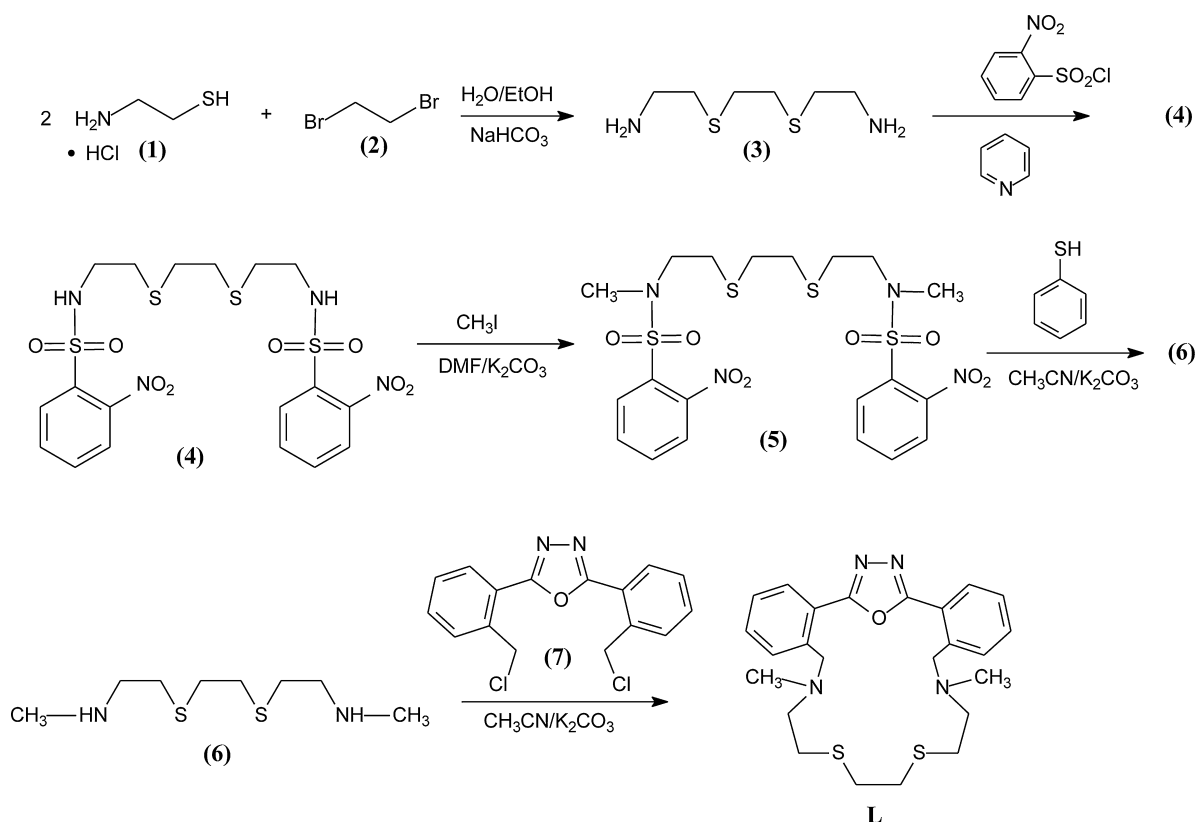
Scheme 1. Scheme of the synthesis of **L**.

amine functions and responds selectively in water via an increase of the fluorescence intensity to Zn(II) also at physiological pH (7.4) [24].

Here we report the synthesis of a new PPD-based chemosensor **L** (Chart 1), in which two thioether groups were inserted together with two amine functions in the macrocycle. We inserted the two S atoms to make the chemosensor suitable for the coordination of soft and heavy metal ions both in organic and aqueous media, enlarging the available toolbox for the detection of metal ions. We also report on the effects of the inclusion of **L** in core–shell water soluble nanoparticles, the so-called PluS Nanoparticles (PluS NPs): silica nanoparticle synthesized with a strategy based on the formation of micelles of Pluronic® F127 in water [25–28]. We have already proposed this strategy to increase the water solubility, the affinity and the signal-to-noise ratio of some chemosensors [29–33]. The extension of this approach to other systems can afford, to our opinion, additional information for the design of a new generation of chemosensors able to investigate the toxic effects of metal ions directly in the compromised environment that is usually an aqueous media, giving analytical answers with high selectivity and sensitivity [34].

2. Results and discussion

2.1. Synthesis

The synthetic pathway used to obtain the ligand **L** is presented in Scheme 1. The 2,11-diaza-5,8-dithiadodecane reagent **6** was obtained in good yield starting from 2-aminoethanethiol **1** and 1,2-dibromoethane **2** and following the procedure reported by Zheng et al. [35] to get the 1,10-diaza-4,7-dithiadecane compound **3** which was then isolated as **3**·2HCl and characterized. The two amine functions of **3** were nosyl-protected using 2-nitrobenzenesulfonylchloride in pyridine to afford in good yield (54%) compound **4**. After purification and characterization **4** was
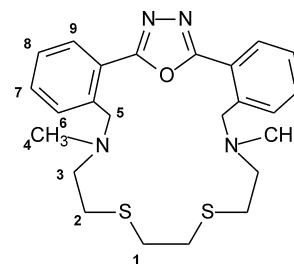
Chart 1. Ligand **L** with atom labelling used in NMR assignments.

reacted with methyliodide in DMF in the presence of an alkaline carbonate base to obtain, in a quantitative yield, **5**. The use of thiophenol in acetonitrile in the presence of an alkaline carbonate base allows the removal of the nosyl amine-protective group and the obtainment of **6**. It was purified in ethanol by precipitation with perchloric acid to obtain the **6**·2HClO$_4$ salt that also allows an easier storage. The heteroaromatic scaffold 2,5-bis[2-(chloromethyl)phenyl][1,3,4]oxadiazole **7** was synthesized as previously reported [23,36].

The final compound **L** was obtained reacting **6**·2HClO$_4$ and **7** in a 1 + 1 cyclization scheme in the presence of an alkaline carbonate base. The cyclization occurs in high yield and **L** was easily purified from the crude products by chromatography and crystallization from hot water/ethanol (80:20, v/v).

2.2. Solution studies

2.2.1. UV–vis and fluorescence of **L** in water:ethanol solutions

The photochemical properties of **L** as a function of the pH were firstly investigated in a protic water:ethanol 1:1 (v/v) solution because of its limited solubility in pure H$_2$O. These experiments showed that the ligand is fluorescent in acid media but quenched at basic pH values (Fig. 1). At pH = 2 **L** absorbs at 280 nm
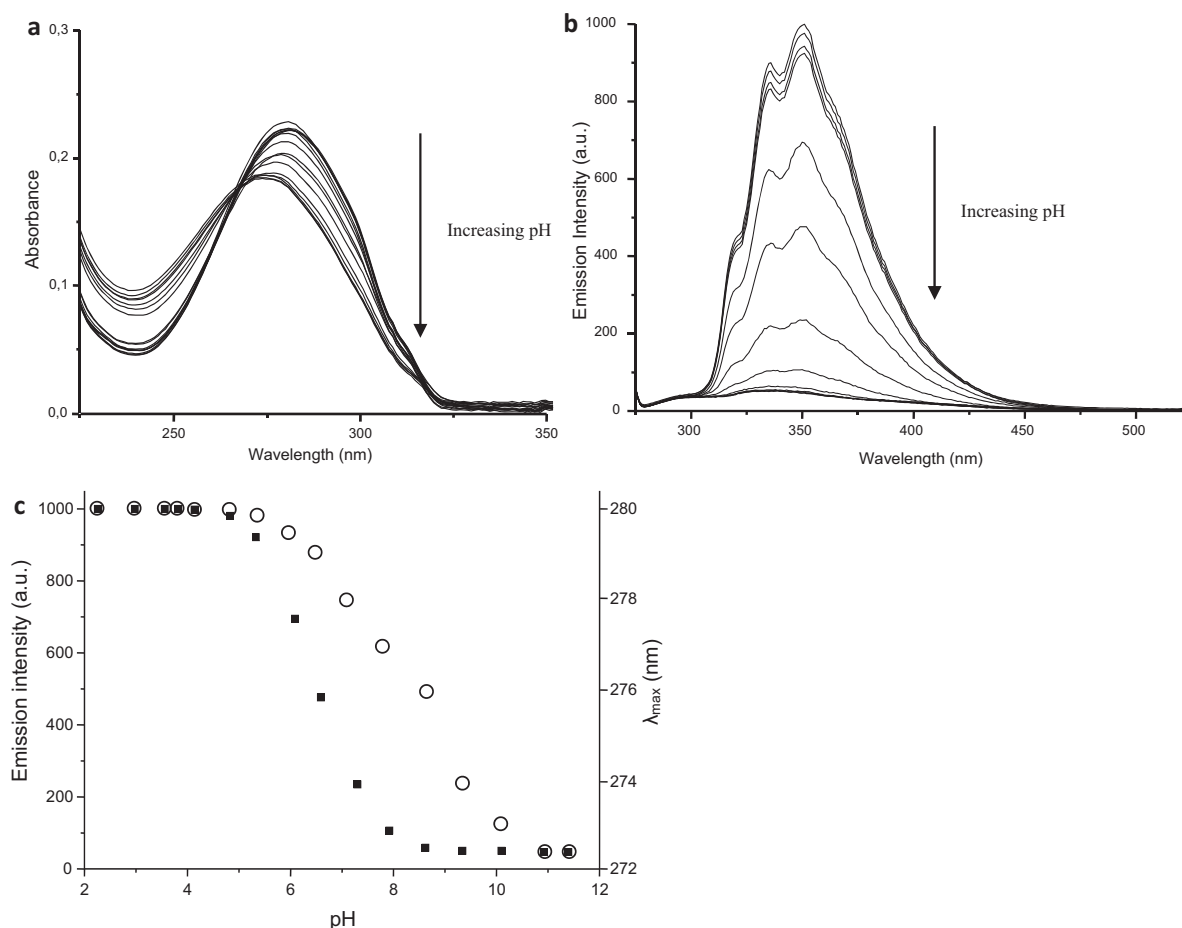
Fig. 1. Absorption (a) and emission (b) spectra of **L**, and (c) trend of the emission intensity (■) and of the absorption λ_{max} (○) of **L** as a function of pH in water. Conditions: [**L**] = 1.5×10^{-5} M; λ_{ex} = 270 nm.

(ε = 14,300 dm^3 mol^{-1} cm^{-1}) and presents a fluorescence emission at 350 nm (Φ = 0.17), that previous theoretical studies on the PPD fragment attributed to a twisted intramolecular charge transfer (TICT) excited state [37]. At pH = 12 the absorption peak undergoes a small blue shift to 273 nm, and the fluorescence was completely quenched. In particular, the drop in fluorescence emission starts at pH 5 while at pH 8 the emission is already completely quenched. This means that at pH < 5 the two amines are protonated, at pH > 8 one of them is deprotonated, and considering the trend of λ_{max} as a function of the pH (Fig. 1c), it is possible to establish that the second amine is deprotonated only at pH > 10. This behaviour has been observed also in similar ligands containing the PPD fluorophore [23,24]. Taken together, all these results indicate that the emission of **L** is regulated by a photo-induced electron transfer (PET) process from the lone pairs of the amine functions to the HOMO of the excited fluorophore. In fact, at acid pH, where both the amines are protonated, the PET process cannot take place and the excited state is emissive; on the contrary, by the deprotonation of the first ammonium group, the PET can occur and the excited state is quenched. On the other hand, the fact that in acid media the ligand is fluorescent means that the two sulphur atoms are not able to quench the PPD.

2.2.2. Photophysical and metal ion binding properties of **L** in acetonitrile solutions

In the aprotic acetonitrile solvent, the absorption spectrum of **L** shows a band at 271 nm (ε = 14,900 dm^3 mol^{-1} cm^{-1}), and no fluorescence could be observed because of the PET process from the lone pairs of the two amine functions. Reasonably, in

these conditions it is possible to predict that the coordination of a suitable metal ion involving the macrocyclic moiety should affect the emission intensity by preventing the PET and switching ON the emission. In addition, the OFF-ON fluorescence signal variation induced by the metal ion coordination should result maximized in this medium with respect to the protic mixed solvent discussed above where **L** is emitting in a large range of pH including the neutrality. However, it has to be considered that the coordination of the metal ion by the donor atoms can also induce constrains in the PPD conformation, and this could also affect the emission properties influencing the TICT state. Moreover, metal coordination can also introduce additional non-radiative deactivation pathways, such as the so-called heavy atom effect. In order to test the behaviour of **L** towards Ca(II), Ba(II), Cu(II), Ag(I), Zn(II), Cd(II), Hg(II) and Pb(II) spectrophotometric and spectrofluorimetric titrations were carried out in this solvent. Ca(II) and Ba(II) did not affect the **L** spectra, probably because they are not complexed by **L**, while Cu(II), Zn(II), Cd(II), Pb(II), Hg(II) and Ag(I) form a not fluorescent M**L** species and a fluorescent M$_2$**L** species. As an example, by addition of Pb(II) ions to a solution of **L** in acetonitrile, the absorption band at 271 increases in ε and undergoes a slight red shift up to 277 nm, and the intensity emission at 350 nm shows a high increase. Both absorption and emission spectra reach the invariance with the addition of two equivalents of Pb(II) ions. In particular, examining the trend of the emission at 350 nm as a function of the added equivalents of Pb(II), we can observe that the increase of the fluorescence starts after the addition of the first one and reaches its maximum at 2 equiv. (Fig. 2). This means that (i) the ligand can bind two equivalents of Pb(II) and (ii) the first Pb(II) does not affect the fluorescence emission
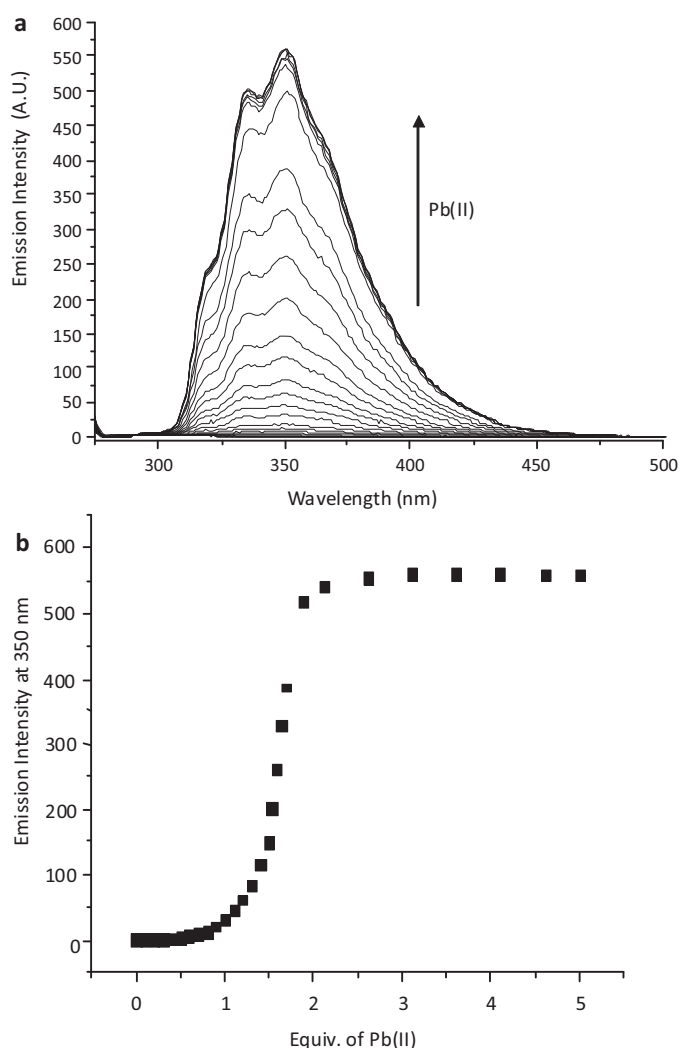
a

b

Fig. 2. Spectrofluorimetric titration (a) of **L** with $Pb(ClO_4)_2$ in acetonitrile and (b) trend of the emission at 350 nm. Conditions: $[\mathbf{L}] = 2 \times 10^{-6}$ M; $[Pb^{2+}] = 0$–1×10^{-5} M; $\lambda_{ex} = 270$ nm.

Table 1

Association constants[a] ($\log K$) of selected metal ions (M = Cu(II), Zn(II), Ag(I), Cd(II) and Hg(II)) to ligand **L** in acetonitrile solution at 298 K determined by fluorescence titration.

Reaction	Log K				
	Cu(II)	Zn(II)	Ag(I)	Cd(II)	Hg(II)
L + M = LM	7.2(3)[a]	7.5(3)	4.06(3)	7.3(6)	6.4(2)
LM + M = LM₂	3.4(3)	6.4(2)	–	3.5(3)	4.3(2)

[a] Values in parentheses are the standard deviations on the last significant figure.

while the second one does. This fluorescent behaviour is similar for all the studied cations for which we have also determined the complexation constants (Table 1) with the exception of Pb(II) that presents such an high affinity to make impossible a reliable quantification with a direct titration. Also Hg(II) shows a rather large association constant ($\log K_{11} = 6.4 \pm 0.2$ and $\log K_{21} = 4.3 \pm 0.2$), but with a much lower enhancement factor similarly to Cu(II), Zn(II) and Cd(II). On the contrary, the silver ions were the ones presenting the lower affinity ($\log K_{11} = 4.06 \pm 0.03$) and the $Ag_2\mathbf{L}$ species could be observed only in the presence of a great excess of metal ion and again with a limited enhancement factor. As already mentioned Pb(II) seems to form the more stable complexes in acetonitrile and, in order to possibly quantify this qualitative evidence, we
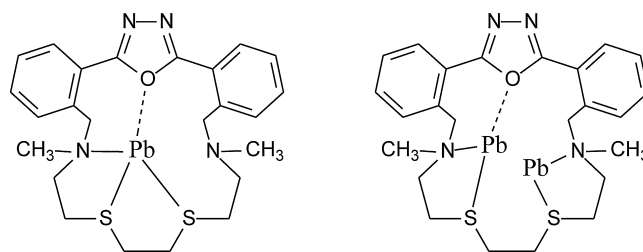
Scheme 2. Proposed coordination models of **L** for the mono- and the di-nuclear Pb(II)-**L** species in acetonitrile solution. The drawings of the complexes are only partial, as other species coordinating at the remaining sites of M(II) are not specified.

performed competition experiments adding increasing amounts of metal ions to a solution containing $Pb_2\mathbf{L}$, following the titration both *via* fluorescence and ^{1}H NMR. However, the addition of 2 equiv. of Cu(II), Zn(II) and Cd(II) still did not affect the emission of the $Pb_2\mathbf{L}$ species preventing the determination of its association constant. It is also worth mentioning that Cu(II), Zn(II), Cd(II) and Pb(II) induce the highest emission enhancements (Table 2) and this could be ascribed to the reasonable greater involvement of the amine functions in the coordination of such metal ions thus more efficiently preventing the PET effect.

2.2.3. NMR studies in acetonitrile solutions

^{1}H NMR studies were performed in order to elucidate the behaviour of **L** in the coordination of the ions. The ^{1}H NMR spectrum of **L** in acetonitrile-d_3 shows five aliphatic and four aromatic resonances (Fig. 3a): a singlet at $\delta = 2.23$ ppm integrating 6 protons attributed to the resonance of H4 (H4, 6H), a singlet at $\delta = 2.46$ ppm (H1, 4H), two symmetrical multiplets at $\delta = 2.50$ and $\delta = 2.60$ ppm (H2 and H3, 8H), a singlet at $\delta = 4.04$ ppm (H5, 4H), a multiplet at $\delta = 7.45$–7.65 ppm (H6, H7 and H8, 6H) and a double doublet at $\delta = 7.99$ ppm (H9, 2H), indicating a C_{2v} symmetry, mediated on the NMR time scale. Upon addition of one equivalent of Pb(II) the ^{1}H NMR spectrum exhibits the broadening and the downfield-shift of all of the aromatic and aliphatic resonances, with the sharp singlet of the benzylic protons (H5) splitting in two very broad signals (Fig. 3a). This suggests that the coordination of the first Pb(II) ion involves most of the donor atoms of the macrocycle, giving rise to a complex in slow exchange on the NMR time scale. The addition of the second equivalent of Pb(II) induces a sharpening and a further downfield shift of all resonances and in particular of H3, that also splits in two distinct resonances, and of one H5, both belonging to the C atom in α-position to the amine function. The resonance of the methyl group (H4) splits in two well defined singlets at $\delta = 2.75$ and $\delta = 2.73$ ppm (Fig. 3a), the ethylene chains give a complex pattern of signals and the benzylic CH_2 signals (H5) split into two distinct signals: a double doublet of doublets at $\delta = 4.31$ and a double triplet $\delta = 5.11$ ppm. This indicates, in agreement with the spectrophotometric measurements, the binding of a second Pb(II) ion and the formation of a dinuclear Pb(II) species. The stiffening of the complex makes all the protons not equivalent on the NMR time scale and their further downfield shift suggests that in this species, all the four donor atoms are strongly involved in the metal coordination. All the PPD resonances exhibit a downfield shift which is more marked for H9 and, although shifts are not large, a partial involvement of PPD in the stabilization of Pb(II) could be envisaged. A possible coordination model for **L** in the mono- and the di-nuclear Pb(II)-**L** species in acetonitrile solution is reported in Scheme 2.

Fig. 3b shows the spectra recorded after the addition of 1 and 2 equiv. of Hg(II). In this case, the addition of the first and the second equivalent of Hg(II) causes the downfield shift of all aliphatic signals, while the aromatic resonances undergo only minimal
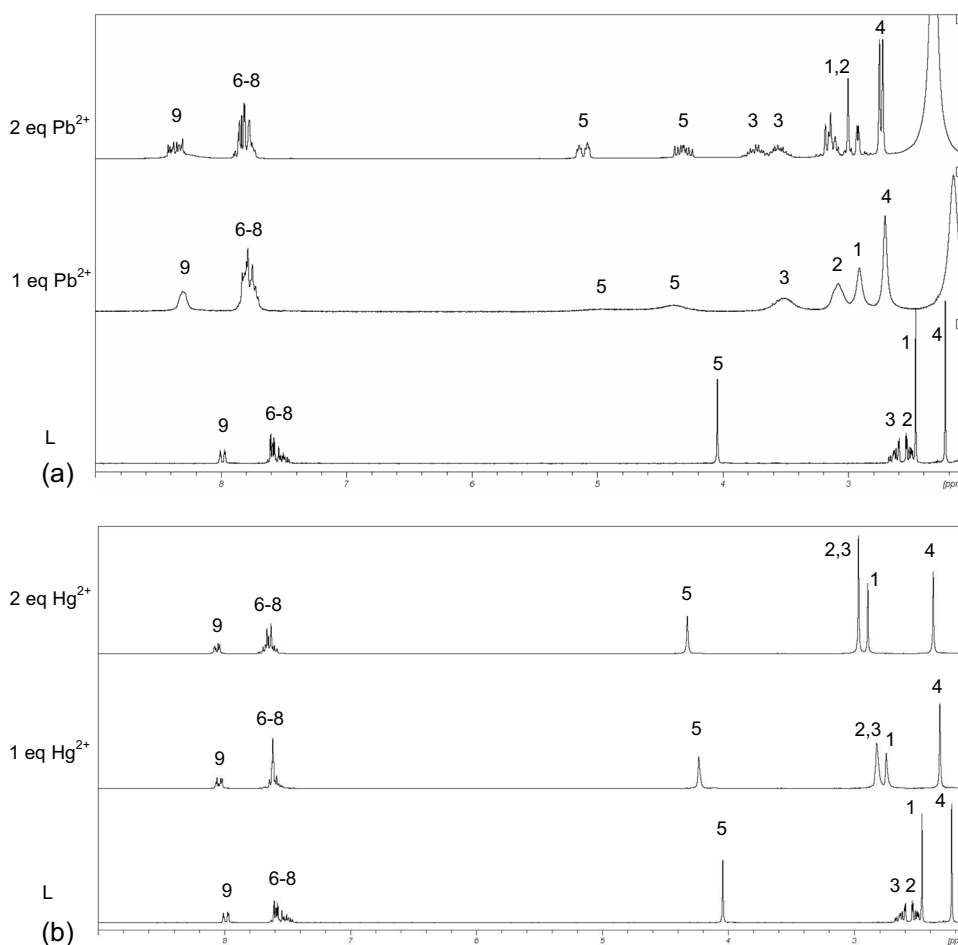
Fig. 3. ^{1}H NMR spectrum of **L** (1.0×10^{-2} mol dm^{-3}) alone and after the addition of (a) 1.0 and 2.0 equiv. of Pb(II) or (b) 1.0 and 2.0 equiv. of Hg(II). All spectra were recorded in CD$_3$CN at 298 K.

Table 2
Quantum yield Φ_f of M$_2$L complexes; M = Cu(II), Zn(II), Ag(I), Cd(II), Hg(II) and Pb(II).

Cu(II)	Zn(II)	Cd(II)	Ag(I)	Hg(II)	Pb(II)
0.053	0.097	0.080	0.025	0.005	0.145

modifications. This suggests that most of the binding donor atoms are involved in the stabilization of the two Hg(II) ions while the PPD unit is not. The higher shift exhibited by the resonances attributed to protons H1 and H2, belonging to the group in α-position to the S groups, with respect to H3 and H4, belonging to the group in α-position to the N group, suggests that the two sulphur atoms give an higher contribution to the stabilization of this thiophilic metal ion.

The ^{1}H NMR spectra carried out with Ag(I), Zn(II) and Cd(II) showed a similar behaviour with respect to the one observed for Hg(II). The addition of Ag(I) reveals the higher involvement of S groups in the stabilization of both Ag**L** and Ag$_2$**L** species because H1 and H2, exhibit higher downfield shift with respect to H3 and H4. On the contrary, the addition of Zn(II) shows the higher shift of H3 and H4 than H1 and H2 resonances denoting the higher involvement of the amine groups in its stabilization.

Considering the Pb(II) species, it is possible to assess that: (i) the Pb**L** complex is fluxional on the NMR time scale and it is not fluorescent; (ii) the Pb$_2$**L** complex is rigid on the NMR time scale and it is fluorescent; (iii) in both mononuclear and dinuclear complexes all the aliphatic functions are involved in the coordination; moreover

the PPD could cooperate in Pb(II) complexation and this could be the reason of its high stability.

On the basis of these elements it is possible to propose the following model for the spectroscopic behaviour of **L** with Pb(II). In the mononuclear complex the soft character of the Pb(II) ion drives it to strongly bind the two sulphur atoms, and probably only one of the amine functions. The presence of a free lone pair in one benzylic amine, as already observed in analogous chemosensors containing the PPD fluorophore [7,24], prevents the emission of the fluorophore due to a PET process. The coordination of the second Pb(II) involves all thioether and amine functions and blocks the ligand in a stiffen conformation, causing the switch-ON of the fluorescence by preventing the PET. A similar involvement of the aliphatic binding groups can be suggested also in other cases and, as a result, the metal complexes showing higher affinity to N than to S such as Zn(II) and Cu(II) are higher emitters than the ones with Ag(I) or Hg(II) which are more thiophilic.

In conclusion, all these NMR results are in agreement with spectrofluorimetric titrations regarding the formation of M**L** and M$_2$**L** species indicating that in the M$_2$**L** species the two aliphatic amines, in addition to the aliphatic thiols, are involved in the coordination of all metal ions and this is the likely reason of the OFF-ON response of the fluorescence.

2.2.4. Use of PluS Nanoparticles

As already mentioned, we have developed a one-pot approach for the synthesis of water-soluble silica core/shell nanoparticles,
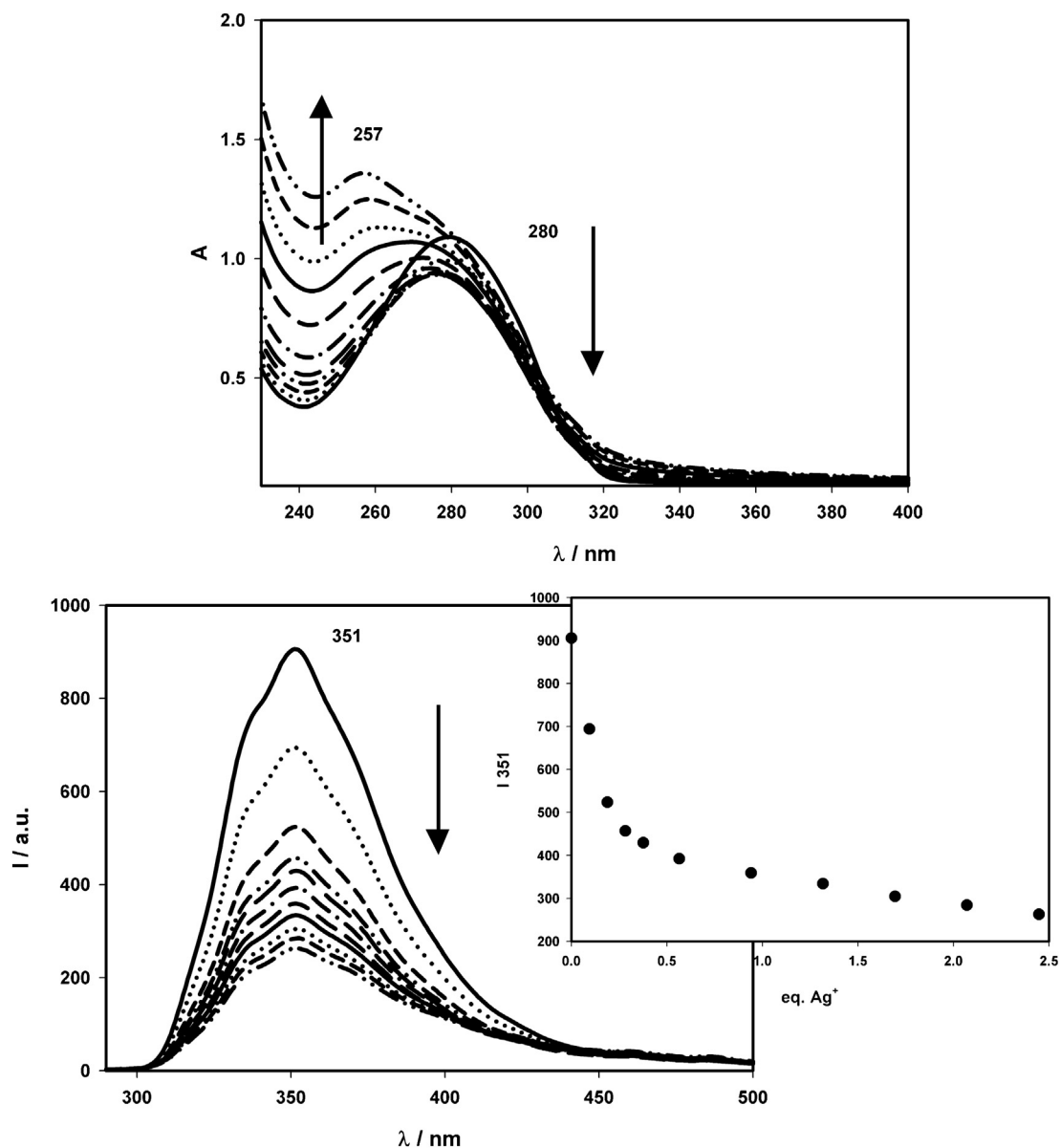
Fig. 4. Variation of the absorption spectrum of **L@NPs** 40:1 in MOPS buffer (pH = 7.4) after the addition of increasing amounts of AgNO$_3$ 1.0 × 10^{-2} M; emission spectra (λ = 270 nm) with the trend at 351 nm.

named PluS Nanoparticles, based on the formation of micelles of Pluronic® F127 in water. The final material is a nanostructure characterized by a high water solubility, stability, and, when properly doped with suitable dyes, brightness. Most interestingly, we have also demonstrated the possibility of hosting inside this multicompartment system water-insoluble functional molecules, such as dyes [38], drugs, photoswitches, and chemosensors [29,31,32]. In particular, in this latter case we proved the possibility, with this strategy, to increase the water solubility, the affinity and the signal-to-noise ratio of the chemosensors. For this reason, in the attempt to host **L** inside the Plus NPs, we added an increasing amount of a 4.9 × 10^{-4} M solution of the chemosensor in CH$_3$CN to a 1.0 × 10^{-6} M water suspension of NPs buffered at pH 7.4 with MOPS. Up to the addition of ca 100 equiv., the system did not show any form of aggregation, the only structure visible with dynamic light scattering (DLS) is, in fact, attributable to the NPs having a hydrodynamic diameter of ca 22 nm, with a very high monodispersity. By contrast, the addition of even small aliquots of **L** to a water solution in absence of NPs leads to the formation of a

precipitate clearly visible also with naked eye; DLS experiments in this case clearly showed the formation of aggregates having a diameter of ca 50 nm and high polydispersity. The absorption maximum of the system **L@NPs** was at 280 nm, while the fluorescence band peaked at 351 nm, with a quantum yield of 0.033 and a mean excited state lifetime of 0.3 ns. Interestingly, a rather high fluorescence anisotropy (0.13) was observed in this case, giving additional evidence for the inclusion of **L** inside a larger structure, as already observed in similar cases with the same kind of nanoparticles [30,31,38,39]. For all the following experiments, we choose the use of a suspension of NPs hosting, in the average, 40 molecules of **L** per nanoparticle, in order to exclude any possible precipitation of the chemosensor. We tested the effect of the addition of the same set of metal ions previously used in acetonitrile, i.e., Ca(II), Ba(II), Cu(II), Ag(I), Zn(II), Cd(II), Hg(II) and Pb(II), both as their nitrate and perchlorate salts. The observed behaviour in these conditions, that was independent on the anion, was dramatically different from the one in acetonitrile. We could in fact detect emission changes only upon addition of Ag(I) and Hg(II) ions (Figs. 4 and 5, respectively). In
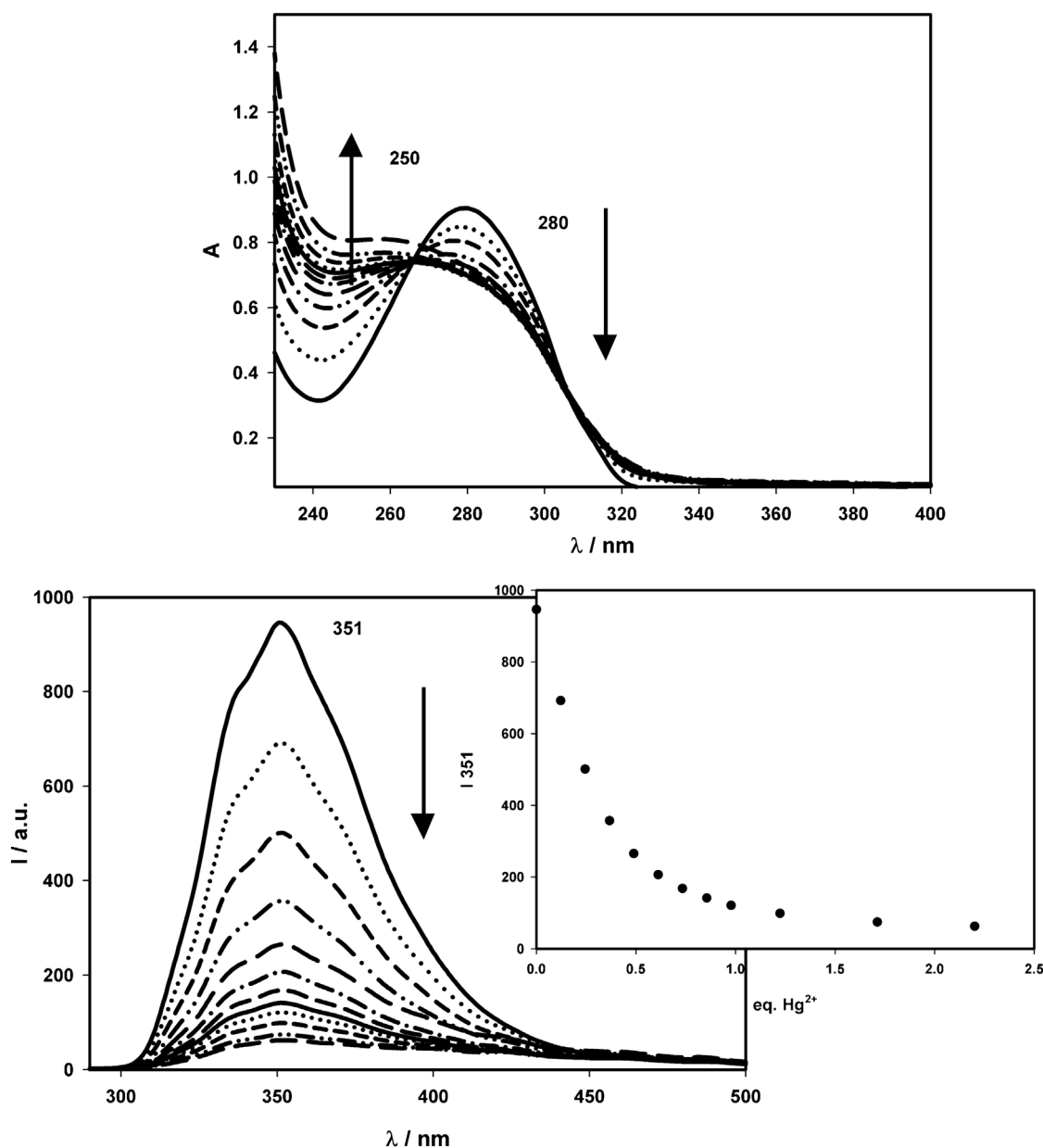
Fig. 5. Variation of the absorption spectrum of **L@NP** 40:1 in MOPS buffer (pH = 7.4) after the addition of increasing amounts of Hg(NO$_3$)$_2$·H$_2$O 1.3 × 10^{-2} M; emission spectra (λ = 270 nm) with the trend at 351 nm.

particular, increasing amounts of Hg(II) caused a significant decrease of the fluorescence intensity; from the fitting of the titration curve it was possible to evidence the formation of a complex having a 1:2 M:L stoichiometry (log β_a = 10.0 ± 0.2) with Φ = 0.002 and an excited state lifetime equal to 0.2 ns. Similarly, upon addition of Ag(I) ions, it was also possible to observe a decrease of the emission intensity. The species formed possesses a 1:2 M:L stoichiometry (log β_a = 9.7 ± 0.2) with a fluorescence quantum yield = 0.001 and an excited state lifetime equal to 0.1 ns. To verify if the different stoichiometry observed in these conditions could be attributed only to the different solvent or, more likely, to the close neighbouring of the ligands when included in the core–shell structure, we performed a new titration experiment in the presence of nanoparticles hosting a lower amount of chemosensor (2 molecules per NP). Interestingly, also in these conditions we observed a dramatic decrease of the fluorescence

intensity, which could, however, be fitted only assuming a 1:1 stoichiometry (log K_a = 5.42 ± 0.04). This difference clearly indicates that the local concentration of **L** inside the nanoparticles has a fundamental role in the determination of the complex stoichiometry. The lack of evidence for the complex having a 2:1 M:L stoichiometry inside the NPs can be accounted for the high concentration of the ligand in this restricted medium, where, on the contrary, the concentration of the more hydrophilic free metal ion is low.

It is worth to underline that, when hosted by the PluS NPs, **L** in water solution is much more selective than in acetonitrile. In fact, its photophysical properties change only upon the addition of Ag(I) and Hg(II). Moreover, it has to be noted that for the first time, to our knowledge, it was possible to control the stoichiometry of the formed complex upon changing the number of ligands per nanoparticle. We propose this approach as a new additional tool

to control the affinity, specificity and photophysical response for a next generation of chemosensors.

3. Conclusion

We have reported here the synthesis of a new PPD-based chemosensor presenting two thioether groups together with two amine functions in the macrocycle to make it suitable for the coordination of soft and heavy metal ions. We have performed the photophysical characterization and the study of its metal ion binding properties both in acetonitrile and in buffered water, in the latter case after hosting the chemosensor inside PluS Nanoparticles. NMR spectra obtained in acetonitrile helped us to elucidate the different complexation processes involved in the binding of various metal cations in acetonitrile. As already reported for other species, the inclusion of **L** inside the NP structure leads to a higher water solubility, allowing to perform the complexation experiment also in this widespread and most interesting solvent from an application point of view. The interaction of the chemosensor with the NP induces also other advantages such as an higher selectivity. In fact, while in CH_3CN **L** was able to complex a large number of cations, **L@NP** was responsive only to the presence of Ag(I) and Hg(II). Moreover, as already observed in other cases, the use of these nanostructures leads to an high affinity towards the mercury. Finally, due to the high degree of loading reachable in the NPs, it was demonstrated, for the first time to our knowledge, the possibility to control the stoichiometry of the formed complex upon changing the number of ligands per nanoparticle. To our opinion, this possibility can be seen as an additional tool for the tuning of the affinity and selectivity of the chemosensor that could be of great interest for the design of more and more efficient systems.

4. Experimental

4.1. General methods

^{1}H NMR and ^{13}C NMR spectra were recorded at 298 K on a Bruker Avance instrument, operating at 200.13 and 50.33 MHz, respectively. For the spectra recorded in D_2O, the peak positions are reported with respect to HOD (4.75 ppm) for ^{1}H NMR spectra, while dioxane was used as reference standard in ^{13}C NMR spectra ($\delta = 67.4$ ppm). For the spectra recorded in $CDCl_3$ the peak positions are reported with respect to TMS. All reagents and solvents used were of analytical grade.

4.2. Synthesis

Compound **L** was obtained following the synthetic procedure reported in Scheme 1. 2,5-Bis[2-(chloromethyl)phenyl][1,3,4]oxadiazole (**7**) was prepared as previously reported [23,36]. All other chemicals were purchased in the highest quality commercially available. The solvents were RP grade, unless otherwise indicated.

4.2.1. 1,10-Diaza-4,7-dithiadecane (**3**)

A solution of 1,2-dibromoethane **2** (18,8 g, 0.1 mol) in ethanol (200 cm^3) was added in an inert atmosphere and dropwise to a solution containing 2-aminoethanethiol dihydrochloride **1**·2HCl (22.7 g, 0.2 mol) and $NaHCO_3$ (16.8 g, 0.2 mol) in pure water (200 cm^3). The mixture obtained was maintained under stirring at a room temperature for 30 min and then it refluxed for 3 h. The solvent was evaporated under vacuum. The resulting yellowish oil was dissolved in ethanol (50 cm^3) and 10% hydrochloric acid was

added dropwise to the resulting solution up to total precipitation of **3**·2HCl as a white solid (8.86 g, 35%).

^{1}H NMR (D$_2$O, 25 °C): $\delta = 3.33$ (t, 4H, $J = 6.6$ Hz), 3.00 (t, 4H, $J = 6.6$ Hz), 2.95 (s, 4H) ppm; ^{13}C NMR (D$_2$O, 25 °C): $\delta = 38.8$, 30.8, 28.4 ppm. Anal. Calcd. for $C_6H_{18}Cl_2N_2S_2$ (%): C 28.46; H 7.16; N 11.06; Found: C 28.5; H 7.2; N 11.1.

4.2.2.
1,10-Bis(2-nitrobenzenesulfonyl)-1,10-diaza-4,7-dithiadecane (**4**)

A solution of 2-nitrobenzenesulfonylchloride (8.2 g, 37.5 mmol) in pyridine (20 cm^3) was added in an inert atmosphere, dropwise to a solution containing **3** (2.65 g, 15 mmol) in pyridine (20 cm^3). The mixture obtained was maintained under stirring at a room temperature for 48 h. The mixture was poured under stirring into cold water (100 cm^3). The resulting precipitate was filtered off and dried under vacuum. The crude product was chromatographed on silica gel (ethyl acetate–hexane 80:20). The eluted fractions were collected and evaporated to dryness, affording **4** as a yellow solid (4.46 g, 54%).

^{1}H NMR (CDCl$_3$, 25 °C): $\delta = 8.15$ (m, 2H), 7.90 (m, 2H), 7.78 (m, 4H), 5.85 (t, 2H, $J = 5.0$ Hz), 3.30 (m, 4H), 2.76 (t, 4H, $J = 6.5$ Hz), 2.69 (s, 4H) ppm; ^{13}C NMR (CDCl$_3$, 25 °C): $\delta = 147.8$, 134.0, 133.3, 133.1, 130.9, 125.5, 43.0, 31.9, 31.7 ppm. MS (m/z): 551.0 (M+H). Anal. Calcd. for $C_{18}H_{22}N_4O_8S_4$ (%): C 39.26; H 4.03; N 10.17; Found: C 39.4; H 4.0; N 10.3.

4.2.3.
2,11-Bis(2-nitrobenzenesulfonyl)-2,11-diaza-5,8-dithiadodecane (**5**)

A solution of methyliodide (2.84 g, 20 mmol) in dry DMF (50 cm^3) was added in an inert atmosphere, dropwise at 0 °C, to a solution containing **4** (5.50 g, 10 mmol) in dry DMF (50 cm^3). The mixture obtained was maintained under stirring at a room temperature for 12 h. The mixture was poured under stirring into cold water (200 cm^3). The resulting yellow precipitate was filtered off and dried under vacuum. The crude product was dissolved in CHCl$_3$ (100 cm^3); the mixture was filtered and the organic solvent was evaporated under vacuum obtaining **5** as a yellow solid in a quantitative yield (5.7 g).

^{1}H NMR (CDCl$_3$, 25 °C): $\delta = 7.96$ (m, 2H), 7.70 (m, 4H), 7.62 (m, 2H), 3.43 (t, 4H, $J = 8.0$ Hz), 2.94 (s, 6H), 2.76 (m, 8H, $J = 8.0$ Hz) ppm; ^{13}C NMR (CDCl$_3$, 25 °C): $\delta = 148.0$, 133.9, 132.0, 131.9, 130.5, 124.2, 49.9, 35.0, 31.9, 30.1 ppm. MS (m/z): 579.1 (M+H). Anal. Calcd. for $C_{20}H_{26}N_4O_8S_4$ (%): C 41.51; H 4.53; N 9.68; Found: C 41.3; H 4.60; N 9.6.

4.2.4. 2,11-Diaza-5,8-dithiadodecane (**6**)

5 (5.78 g, 0.010 mol), thiophenol (6.61 g, 0.060 mol) and K$_2$CO$_3$ (13.8 g, 0.10 mol) were suspended in anhydrous CH$_3$CN (100 cm^3); the mixture was maintained under stirring at a room temperature for 48 h. The solvent evaporated under vacuum. The resulting oil was dissolved in CHCl$_3$ (50 cm^3); the mixture was filtered and the organic solvent was evaporated under vacuum. The crude product was dissolved in ethanol (50 cm^3) and 10% perchloric acid solution was added dropwise to the resulting solution; diethyl ether was added (50 cm^3) up to total precipitation of **6**·2HClO$_4$ as a white solid (1.96 g, 48%).

^{1}H NMR (D$_2$O, 25 °C): $\delta = 3.11$ (t, 4H, $J = 6.5$ Hz), 2.75 (t, 4H, $J = 6.5$ Hz), 2.69 (s, 4H), 2.57 (s, 6H) ppm; ^{13}C NMR (D$_2$O, 25 °C): $\delta = 47.6$, 32.6, 30.4, 26.8 ppm. MS (m/z): 409.0 (M+H). Anal. Calcd. for $C_8H_{22}Cl_2N_2O_8S_2$ (%): C 23.48; H 5.42; N 6.84; Found: C 23.3; H 5.50; N 6.8.

4.2.5. 9,12-Dimethyl-9,12,27,28-tetraaaza-15,18-dithia-29-oxatetracyclo[24.2.1.0²,⁷.0²⁰,²⁵]-enneicosa-2,4,6,20,22,24,26,28¹-octaene (**L**)

Over a period of 4 h, a solution of **7** (958 mg, 3 mmol) in $200\,cm^3$ of anhydrous CH_3CN was added to a suspension of **6**·2HClO$_4$ (1.23 g, 3 mmol) and K_2CO_3 (4.15 g, 30 mmol) in $200\,cm^3$ of anhydrous CH_3CN, at reflux under nitrogen. The reaction mixture was maintained at reflux for further 12 h. Subsequently, the solvent was evaporated under vacuum and the solid obtained washed with $CHCl_3$ ($100\,cm^3$). The organic layer was evaporated under reduced pressure and the solid was chromatographed on neutral alumine ($CHCl_3$). The eluted fractions were collected and evaporated to dryness. The product was further purified by crystallization in ethanol:water 9/1 (v/v) affording **L** as a white solid (790 mg, 58%).

^{1}H NMR ($CDCl_3$, 25 °C): $\delta = 8.00$ (m, 2H), 7.49 (m, 6H), 4.07 (s, 4H), 2.74 (m, 8H), 2.66 (s, 4H), 2.24 (s, 6H); ^{13}C NMR ($CDCl_3$, 25 °C): $\delta = 163.7, 139.2, 132.0, 130.9, 129.6, 127.7, 123.6, 60.3, 58.3, 42.1, 32.4, 29.4$ ppm; MS (m/z) (ESI): 455.2 (M+H$^+$); Anal. Calcd. for $C_{24}H_{30}N_4OS_2$ (%): C 63.40, H 6.65, N 12.32; Found: C 63.4, H 6.7, N 12.3.

4.2.6. Synthesis of PluS Nanoparticles

Plus NPs were synthesized as already reported [39]. 1.000 g of Pluronic F127 and 0.680 g of NaCl were solubilized under magnetic stirring with 15.65 mL of acetic acid 1.0 M for 1 h. Tetraethyl orthosilicate (TEOS, 1780 μL, 7.97 mmol) was then added to the resulting aqueous homogeneous solution, followed by chlorotrimethylsilane (TMSCl, 100 μL, 0.8 mmol) after 3 h. The mixture was stirred for 48 h at 25 °C. The NPs suspension was dialyzed versus water on a precise amount of nanoparticles solution (15.00 mL) finally diluted to a total volume of 50 mL with water (concentration 20 μM) [38].

4.3. Photophysical measurements

Absorption spectra were recorded on a Perkin-Elmer Lambda 45 and on a Varian Cary-100 spectrophotometer equipped with a temperature control unit. For the fluorescence spectroscopy measurements, uncorrected emission and corrected excitation spectra were obtained with a Perkin-Elmer LS 55 spectrofluorimeter. Luminescence quantum yields (uncertainty ±15%) were determined using naphthalene in cyclohexane ($\Phi = 0.036$). In order to allow comparison of emission intensities, corrections were performed for instrumental response, inner filter effects, and phototube sensitivity [40]. Values of $\log K_a$ were obtained by fitting spectrophotometric and spectrofluorimetric data with SPEC-FIT/32, a global analysis software. TCSPC (time-correlated single photon counting) experiments (excitation laser $\lambda = 280$ nm) were performed with an Edinburgh FLS920 equipped photomultiplier Hamamatsu R928P connected to a PCS900 PC card. All fluorescence anisotropy measurements were performed on an Edinburgh FLS920 equipped with Glan-Thompson polarizers. Anisotropy measurements were collected using an L-format configuration, and all data were corrected for polarization bias using the G-factor.

Acknowledgements

References

[1] R.A. Bissell, A.P. De Silva, H.Q.N. Gunaratne, P.L.M. Lynch, G.E.M. Maguire, K. Sandanayake, Molecular fluorescent signaling with fluorophore spacer receptor systems – approach to sensing and switching devices via supramolecular photophysics, Chem. Soc. Rev. 21 (1992) 187–195.

[2] A.P. de Silva, D.B. Fox, A.J.M. Huxley, T.S. Moody, Combining luminescence, coordination and electron transfer for signalling purposes, Coord. Chem. Rev. 205 (2000) 41–57.

[3] A.P. de Silva, H.Q.N. Gunaratne, T. Gunnlaugsson, A.J.M. Huxley, C.P. McCoy, J.T. Rademacher, et al., Signaling recognition events with fluorescent sensors and switches, Chem. Rev. 97 (1997) 1515–1566.

[4] L. Prodi, Luminescent chemosensors: from molecules to nanoparticles, New J. Chem. 29 (2005) 20–31.

[5] B. Valeur, I. Leray, Design principles of fluorescent molecular sensors for cation recognition, Coord. Chem. Rev. 205 (2000) 3–40.

[6] C. Lodeiro, J.L. Capelo, J.C. Mejuto, E. Oliveira, H.M. Santos, B. Pedras, et al., Light and colour as analytical detection tools: a journey into the periodic table using polyamines to bio-inspired systems as chemosensors, Chem. Soc. Rev. 39 (2010) 2948–2976.

[7] M. Formica, V. Fusi, L. Giorgi, M. Micheloni, New fluorescent chemosensors for metal ions in solution, Coord. Chem. Rev. 256 (2012) 170–192.

[8] M. Valko, H. Morris, M.T.D. Cronin, Metals, toxicity and oxidative stress, Curr. Med. Chem. 12 (2005) 1161–1208.

[9] T.W. Clarkson, L. Magos, G.J. Myers, The toxicology of mercury – current exposures and clinical manifestations, N. Engl. J. Med. 349 (2003) 1731–1737.

[10] N. Rifai, G. Cohen, M. Wolf, L. Cohen, C. Faser, J. Savory, et al., Incidence of lead-poisoning in young-children from inner-city, suburban, and rural communities, Ther. Drug Monit. 15 (1993) 71–74.

[11] S. Satarug, S.H. Garrett, M.A. Sens, D.A. Sens, Cadmium, environmental exposure, and health outcomes, Environ. Health Perspect. 118 (2010) 182–190.

[12] J.L. Barriada, A.D. Tappin, E.H. Evans, E.P. Achterberg, Dissolved silver measurements in seawater, Trends Anal. Chem. 26 (2007) 809–817.

[13] J.F. Zhang, Y. Zhou, J. Yoon, J.S. Kim, Recent progress in fluorescent and colorimetric chemosensors for detection of precious metal ions (silver, gold and platinum ions), Chem. Soc. Rev. 40 (2011) 3416–3429.

[14] L. Liu, D.Q. Zhang, G.X. Zhang, J.F. Xiang, D.B. Zhu, Highly selective ratiometric fluorescence determination of Ag(+) based on a molecular motif with one pyrene and two adenine moieties, Org. Lett. 10 (2008) 2271–2274.

[15] V.K. Bhardwaj, A.P.S. Pannu, N. Singh, M.S. Hundal, G. Hundal, Synthesis of new tripodal receptors – a 'PET' based 'off-on' recognition of Ag(+), Tetrahedron 64 (2008) 5384–5391.

[16] H.J. Klasen, Historical review of the use of silver in the treatment of burns. I. Early uses, Burns 26 (2000) 117–130.

[17] V. Sambhy, M.M. MacBride, B.R. Peterson, A. Sen, Silver bromide nanoparticle/polymer composites: dual action tunable antimicrobial materials, J. Am. Chem. Soc. 128 (2006) 9798–9808.

[18] K. Matsuda, N. Hiratsuka, T. Koyama, Y. Kurihara, O. Hotta, Y. Itoh, et al., Sensitive method for detection and semiquantification of Bence Jones protein by cellulose acetate membrane electrophoresis using colloidal silver staining, Clin. Chem. 47 (2001) 763–766.

[19] A.T. Wan, R.A.J. Conyers, C.J. Coombs, J.P. Masterton, Determination of silver in blood, urine, and tissues of volunteers and burn patients, Clin. Chem. 37 (1991) 1683–1687.

[20] H.H. Harris, I.J. Pickering, G.N. George, The chemical form of mercury in fish, Science 301 (2003) 1203.

[21] P.B. Tchounwou, W.K. Ayensu, N. Ninashvili, D. Sutton, Environmental exposure to mercury and its toxicopathologic implications for public health, Environ. Toxicol. 18 (2003) 149–175.

[22] M. Mameli, M.C. Aragoni, M. Arca, C. Caltagirone, F. Demartin, G. Farruggia, et al., A selective, nontoxic, OFF-ON fluorescent molecular sensor based on 8-hydroxyquinoline for probing Cd^{2+} in living cells, Chem.-Eur. J. 16 (2010) 919–930.

[23] G. Ambrosi, M. Formica, V. Fusi, L. Giorgi, E. Macedi, M. Micheloni, et al., New family of polyamine macrocycles containing 2,5-diphenyl[1,3,4]oxadiazole as a signaling unit. Synthesis, acid–base and spectrophotometric properties, Org. Biomol. Chem. 8 (2010) 1471–1478.

[24] G. Ambrosi, M. Formica, V. Fusi, L. Giorgi, E. Macedi, M. Micheloni, et al., Efficient fluorescent sensors based on 2,5-diphenyl[1,3,4]oxadiazole: a case of specific response to Zn(II) at physiological pH, Inorg. Chem. 49 (2010) 9940–9948.

[25] D. Genovese, E. Rampazzo, S. Bonacchi, M. Montalti, N. Zaccheroni, L. Prodi, Energy transfer processes in dye-doped nanostructures yield cooperative and versatile fluorescent probes, Nanoscale 6 (2014) 3022–3036.

[26] E. Rampazzo, R. Voltan, L. Petrizza, N. Zaccheroni, L. Prodi, F. Casciano, et al., Proper design of silica nanoparticles combines high brightness, lack of cytotoxicity and efficient cell endocytosis, Nanoscale 5 (2013) 7897–7905.

[27] E. Rampazzo, F. Boschi, S. Bonacchi, R. Juris, M. Montalti, N. Zaccheroni, et al., Multicolor core/shell silica nanoparticles for in vivo and ex vivo imaging, Nanoscale 4 (2012) 824–830.

[28] E. Rampazzo, S. Bonacchi, D. Genovese, R. Juris, M. Montalti, V. Paterlini, et al., Pluronic-silica (PluS) nanoparticles doped with multiple dyes featuring complete energy transfer, J. Phys. Chem. C 118 (2014) 9261–9267.

[29] S. Bonacchi, D. Genovese, R. Juris, M. Montalti, L. Prodi, E. Rampazzo, et al., Luminescent chemosensors based on silica nanoparticles, in: L. Prodi, M. Montalti, N. Zaccheroni (Eds.), Luminescence Applied in Sensor Science, Springer-Verlag Berlin, Berlin, 2011, pp. 93–138.

[30] C. Bazzicalupi, C. Caltagirone, Z.F. Cao, Q.B. Chen, C. Di Natale, A. Garau, et al., Multimodal use of new coumarin-based fluorescent chemosensors: towards highly selective optical sensors for Hg^{2+} probing, Chem.-Eur. J. 19 (2013) 14639–14653.

[31] E. Rampazzo, S. Bonacchi, D. Genovese, R. Juris, M. Sgarzi, M. Montalti, et al., A versatile strategy for signal amplification based on core/shell silica nanoparticles, Chem.-Eur. J. 17 (2011) 13429–13432.

[32] E. Oliveira, D. Genovese, R. Juris, N. Zaccheroni, J.L. Capelo, M.M.M. Raposo, et al., Bioinspired systems for metal-ion sensing: new emissive peptide probes based on benzo[d]oxazole derivatives and their gold and silica nanoparticles, Inorg. Chem. 50 (2011) 8834–8849.

[33] M. Montalti, L. Prodi, E. Rampazzo, N. Zaccheroni, Dye-doped silica nanoparticles as luminescent organized systems for nanomedicine, Chem. Soc. Rev. 43 (2014) 4243–4268.

[34] M. Helle, E. Rampazzo, M. Monchanin, F. Marchal, F. Guillemin, S. Bonacchi, et al., Surface chemistry architecture of silica nanoparticles determine the efficiency of in vivo fluorescence lymph node mapping, ACS Nano 7 (2013) 8645–8657.

[35] Q.Y. Zheng, C.F. Chen, Z.T. Huang, A facile method for synthesis of calix 4 crowns containing nitrogen and sulfur atoms, J. Chem. Res. (1999) 212–213.

[36] S.H. Mashraqui, S. Sundaram, T. Khan, A.C. Bhasikuttan, Zn^{2+} selective luminescent "off-on" probes derived from diaryl oxadiazole and aza-15-crown-5, Tetrahedron 63 (2007) 11093–11100.

[37] D.S. Biradar, B. Siddlingeshwar, S.M. Hanagodimath, Estimation of ground and excited state dipole moments of some laser dyes, J. Mol. Struct. 875 (2008) 108–112.

[38] E. Rampazzo, S. Bonacchi, R. Juris, M. Montalti, D. Genovese, N. Zaccheroni, et al., Energy transfer from silica core–surfactant shell nanoparticles to hosted molecular fluorophores, J. Phys. Chem. B 114 (2010) 14605–14613.

[39] G. Valenti, E. Rampazzo, S. Bonacchi, T. Khajvand, R. Juris, M. Montalti, et al., A versatile strategy for tuning the color of electrochemiluminescence using silica nanoparticles, Chem. Commun. 48 (2012) 4187–4189.

[40] A. Credi, L. Prodi, Inner filter effects and other traps in quantitative spectrofluorimetric measurements: origins and methods of correction, J. Mol. Struct. (2014), http://dx.doi.org/10.1016/j.molstruc.03.028.

Biographies

Gianluca Ambrosi is a technician at the University of Urbino; he received his PhD in Chemical and Pharmaceutical Sciences at the University of Urbino after a degree in Chemistry (Università di Bologna). He is an expert in organic synthesis of new ligands able to bind metal cations and anions.

Elisa Borgogelli obtained his MSc degree in Chemistry at the University of Bologna; she then got her PhD in Chemical and Pharmaceutical Sciences at the University of Urbino in 2014. Her research activity regards the metal complex-formation properties in solution.

Mauro Formica attended the University of Messina and graduated in chemistry in 1991 with a 110/110 score. He was awarded with a fellowship position of the National Research Council lasting one year. In 1998 he obtained his PhD degree in Chemical and Pharmaceutical Sciences at the University of Urbino. From 2000 he has a permanent position as researcher of Inorganic Chemistry at the University of Urbino. His main research interests are focused on synthetic macrocyclic compounds, metal complexes, and solution equilibrium studies.

Vieri Fusi is an associate professor of General and Inorganic Chemistry at the University of Urbino; he got his degree in Chemistry and his PhD in Chemical Sciences at the University of Firenze. He is an expert in Supramolecular and Coordination Chemistry, his research activity mainly focussing on the synthesis of new ligands, most of them having a macrocyclic skeleton, and on the study of their metal complex-formation properties. Recent interests center on the synthesis of binding units and metal-complexes behaving as metallo-receptors for the recognition, sensing, signalling, sequestration, transport, dosage, and/or activation of biological and environmental substrates.

Luca Giorgi graduated in Chemistry at the University of Bologna (Italy) in 1996 with a 110/110 score. In 1998 he moved at the University of Urbino (Italy) with a fellowship grant of Sigma-Tau (Rome, Italy) lasting two years. In 2003 he obtain the PhD in Chemical and Pharmaceutical Sciences at the University of Urbino. In 2005 he was appointed researcher of Inorganic Chemistry at the same University. Dr. Giorgi research interests focus on the synthesis of macrocyclic compounds, of their metal complexes, and of solution equilibrium studies.

Mauro Micheloni was born in Prato (Italy) in 1949. He attended the University of Florence and graduated in Chemistry in 1973, with the highest score. In 1990 Dr. Micheloni was appointed full professor of Inorganic Chemistry, and moved to the University of Urbino. Prof. Micheloni's research interests focus on synthesis of new ligand molecules, including many macrocyclic compounds and their metal complexes; thermodynamic of protonation and metal complexes formation equilibria; PGM refining and recovery; PGM plating solutions preparation.

Enrico Rampazzo was born in Verona in 1973. He completed his PhD at the University of Padua under the supervision of Prof. Umberto Tonellato and Fabrizio Mancin. He was a FIRB young researcher and a postdoctoral fellow with Luca Prodi and Marco Montalti at the Photochemical Nanosciences Laboratory of the University of Bologna (Italy). He is now a researcher in the same group. His research activity focus on the synthesis of luminescent dyes, sensors and (electro)luminescent systems based on dye doped silica nanoparticles for the development of sensors and labels.

Massimo Sgarzi obtained his MSc degree in Photochemistry and Chemistry of Materials at University of Bologna in 2008. He received his PhD degree in 2014 defending a thesis about the characterization of optical transduction-based molecular systems and nanoparticles for the development of chemical sensors, working with Professor Prodi's group in Bologna. He is currently a postdoctoral fellow in the same laboratory, continuing the work on the photophysical characterization of fluorescent chemosensors and silica nanoparticles for biological and environmental applications.

Nelsi Zaccheroni studied and obtained her PhD in Chemical Sciences (1997) at the University of Bologna (Italy), where she has a permanent position as Assistant Professor in Chemistry since January 1999. She started to approach the study of nanomaterials during the year (1997–98) that she spent as postdoctoral fellow within a TMR-CEE project at the University College of Dublin (Ireland). Her research interests are now mainly focused on luminescent systems for imaging and sensing, both molecular and nanostructured in particular based on silica, metal and core–shell multimaterial nanoparticles.

Luca Prodi is full professor of General and Inorganic Chemistry at the University of Bologna. His research activity is focussed on the synthesis and characterization of luminescent sensors and labels. In this context, he is also actively working on the synthesis and characterization of metal and silica nanoparticles, in order to obtain more efficient sensors and labels mainly for bio-medical applications. He is also inventor of 4 patents and a co-founder of two spin-off companies.